Global Journal of Engineering and Technology Advances
eISSN: 2582-5003
Cross Ref DOI: 10.30574/gjeta
Journal homepage: https://gjeta.com/

(Research Article)

Check for updates

# EFFECT OF FIN GEOMETRY ON THE STABILITY AND AERODYNAMIC PERFORMANCE OF A MODEL ROCKET

Solomon Saiki *, Ayodeji Olaoluwa Alake, Peter Ogoegbunam Onyechi, George Chijioke Okewih and Ayodele Temitope Adekunle

Bola Ahmed Tinubu Centre for space transport and propulsion / national space research and development agency Lagos Nigeria.
* Corresponding Author

Global Journal of Engineering and Technology Advances, 2026, 28(03), 044–052

Publication history: Received on 27 July 2026; revised on 05 September 2026; accepted on 07 September 2026

Article DOI: https://doi.org/10.30574/gjeta.2026.28.3.0236



## ABSTRACT

Fin geometry is the single most design-accessible parameter governing the static stability, drag, and altitude performance of a model rocket, yet it is frequently selected by convention rather than analysis. This paper presents a systematic parametric study of trapezoidal, clipped-delta, and elliptical fin planforms using the Barrowman method for center-of-pressure prediction combined with a wetted-area skin-friction drag model and a simplified one-dimensional powered/coast trajectory estimate. A representative single-stage, three-fin sport model rocket is used as the baseline configuration. Fin aspect ratio, taper ratio, leading-edge sweep angle, and fin count are varied independently, and their effects on static margin, fin drag coefficient, and predicted apogee are quantified. The results show that static margin is comparatively insensitive to aspect ratio once fin count and planform area are fixed, is reduced by increasing taper ratio and sweep angle, and increases nearly linearly with fin count while incurring a corresponding drag penalty. Elliptical fins offer the lowest drag of the three planforms studied at equal area, at a modest cost in static margin. These trends are consolidated into practical fin-design guidance for hobby and student rocketry.

**Keywords:** Model Rocket, Fin Geometry, Barrowman Equations, Static Margin, Center of Pressure, Aerodynamic Drag, Aspect Ratio, Rocket Stability.

## 1 INTRODUCTION

Model rocketry provides an accessible and low-cost platform for studying flight vehicle aerodynamics, and the design of the aft fin assembly remains the primary means by which amateur and student designers control static stability. A rocket is statically stable when its center of pressure (CP) lies aft of its center of gravity (CG); the axial separation between these two points, expressed in body diameters ("calibers"), is termed the static margin. Because the airframe and nose cone typically contribute a fixed, comparatively small aerodynamic moment, the fins dominate the placement of the CP, and small changes in fin planform, span, or sweep can shift the static margin substantially [1], [2].

The relationship between fin geometry and aerodynamic performance is well established in principle but is rarely explored quantitatively at the level of an individual student or hobby project, where fin shapes are often selected by tradition (e.g., a simple trapezoid) rather than by a documented trade study. Beyond stability, fin geometry also governs a non-trivial fraction of total vehicle drag through skin friction and interference effects, which in turn affects the altitude the rocket can reach for a given motor impulse [3], [4].

This paper develops a self-contained analytical and computational framework, based on the classical Barrowman method [1], [2] together with a semi-empirical wetted-area drag model [3], [4], to quantify how four fin-geometry variables — aspect ratio, taper ratio, leading-edge sweep angle, and fin count — affect (i) static margin, (ii) fin parasite drag coefficient, and (iii) predicted apogee, for a representative single-stage sport model rocket. A comparison between trapezoidal, clipped-delta, and elliptical fin planforms of equal area and span is also presented. The intent is to translate first-principles aerodynamic theory into concrete, checkable design guidance of the kind a builder can apply directly.

The remainder of the paper is organized as follows. Section II reviews the governing Barrowman equations for fin normal-force slope and center-of-pressure location. Section III presents the drag and trajectory models used to estimate fin drag and apogee. Section IV describes the baseline rocket configuration and the parametric-study methodology. Section V presents and discusses the results. Section VI consolidates the findings into design guidance, and Section VII concludes the paper.

## 2 THEORETICAL BACKGROUND: THE BARROWMAN METHOD

The Barrowman method [1], [2] gives closed-form expressions for the normal-force-coefficient slope and center of pressure of a slender, subsonic, finned vehicle at small angle of attack, by summing the independent contributions of the nose, any transitions, and the fins. For a nose cone of normal-force-coefficient slope C_Nα,n = 2 (a standard result for a slender pointed nose) located with its own center of pressure a distance X_cn from the nose tip, and a set of N_f trapezoidal fins mounted at the aft body, the fin contribution to normal-force slope is given by (1), where K_fb is the fin–body interference factor of (2), s is the fin semi-span, d is the body diameter, C_r and C_t are the root and tip chords, and l_m is the mid-chord sweep distance measured parallel to the body axis [1], [2].

$$C_{N_\alpha,\,f} = K_{fb}\left[\frac{4\,N_f\,(s/d)^2}{1+\sqrt{1+\left(\dfrac{2l_m}{C_r+C_t}\right)^2}}\right] \quad (1)$$

$$K_{fb} = 1+\frac{r}{s+r} \quad (2)$$

Here r is the body radius at the fin root. The fin geometry variables C_r, C_t, s, and l_m are illustrated in Figure 1.

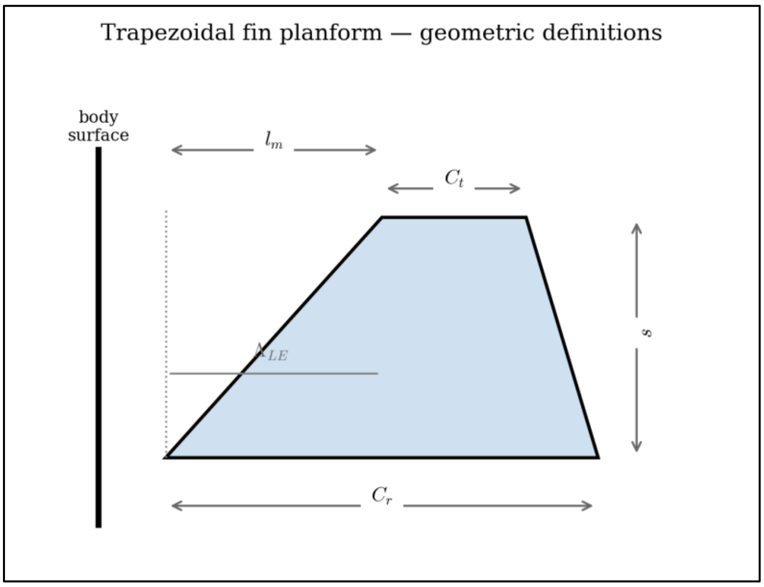


**Figure 1: Trapezoidal fin planform showing the geometric variables used throughout this study: root chord C_r, tip chord C_t, semi-span s, mid-chord sweep length l_m, and leading-edge sweep angle Λ_LE.**

The fin center of pressure, measured parallel to the body axis from the fin root leading edge, is given by (3). The overall vehicle center of pressure is then the normal-force-weighted average of the nose and fin contributions, (4), where X_r is the axial distance from the nose tip to the fin root leading edge.

$$\bar{X}_f = \frac{l_m}{3}\left(\frac{C_r + 2C_t}{C_r + C_t}\right) + \frac{1}{6}\left(C_r + C_t - \frac{C_r C_t}{C_r + C_t}\right) \quad (3)$$

$$X_{cp} = \frac{C_{N_\alpha,\,n} X_{cn} + C_{N_\alpha,\,f}\left(X_r + \bar{X}_f\right)}{C_{N_\alpha,\,n} + C_{N_\alpha,\,f}} \quad (4)$$

Finally, the static margin is the axial separation between X_cp and the center of gravity X_cg, normalized by body diameter, as in (5). A commonly cited rule of thumb for hobby rocketry recommends a static margin between 1 and 2 calibers; values below 1 caliber risk marginal or unstable flight, while excessively large margins increase weathercocking into wind [3], [5].

$$SM = \frac{X_{cp} - X_{cg}}{d} \quad (5)$$

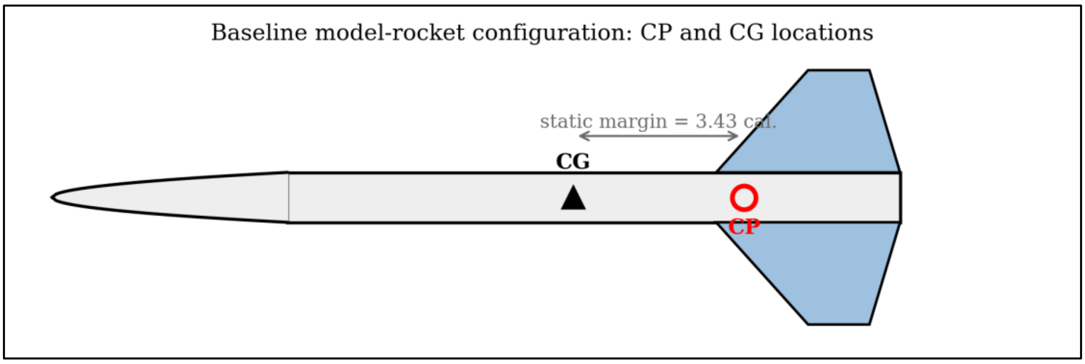


**Figure 2: Baseline rocket configuration showing the predicted center of pressure (CP) and the assumed center of gravity (CG); the axial separation is the static margin.**

## 3 AERODYNAMIC DRAG AND TRAJECTORY MODEL

Fin parasite drag was estimated using the wetted-area skin-friction method commonly used in model-rocket performance prediction software [4]. The turbulent flat-plate skin-friction coefficient C_f is computed from the Reynolds number based on the fin mean aerodynamic chord $\bar{c}$, as in (6), and the total fin drag coefficient, referenced to the body cross-sectional area A_ref, is obtained from (7), where t/c is the fin thickness ratio and A_fin is the planform area of one fin.

$$C_f = \frac{0.074}{Re^{0.2}}, \qquad Re = \frac{\rho V \bar{c}}{\mu} \quad (6)$$

$$C_{D,\,\mathrm{fins}} = C_f\left(1 + 2\frac{t}{c}\right)\frac{4\,N_f\,A_{fin}}{A_{ref}} \quad (7)$$

This formulation captures the first-order trend of fin drag with planform area, thickness, and fin count, and is used here strictly for relative comparison between fin geometries rather than as an absolute drag prediction; wave drag, interference drag beyond the fin-count factor, and boundary-layer transition effects are not modeled explicitly [3], [4].

To translate drag changes into an altitude-relevant metric, apogee was estimated with a simplified one-dimensional point-mass trajectory model: a constant-thrust powered phase (motor total impulse divided by burn time) is integrated together with quadratic aerodynamic drag and weight using a fixed-step numerical (Euler) integration, followed by an unpowered coast to zero velocity. This model is deliberately simplified relative to full six-degree-of-freedom simulators such as OpenRocket [4]; it is used only to illustrate the relative sensitivity of apogee to fin-drag changes, not to predict absolute flight altitude for a specific motor.

Fin aspect ratio, a purely geometric quantity, is defined in (8) as the ratio of the square of the semi-span to the fin planform area, equivalently twice the span divided by the sum of root and tip chords.

$$AR = \frac{s^2}{A_{fin}} = \frac{2s}{C_r + C_t} \quad (8)$$

## 4 BASELINE CONFIGURATION AND METHODOLOGY

The parametric study is built around a representative single-stage, three-fin sport model rocket of the size and mass class commonly used in introductory rocketry (comparable to an Estes Alpha-class airframe), summarized in Table I. This configuration was chosen because it is physically realizable with commonly available hobby materials (balsa or basswood fins, cardboard/phenolic body tube) and because its baseline static margin (computed below) falls within the commonly recommended stability range, providing a realistic starting point from which to perturb individual fin variables [3], [5].

**Table 1: Baseline Rocket and Fin Parameters**

| Parameter | Symbol | Value |
|---|---|---|
| Body diameter | d | 24.4 mm |
| Nose length (tangent ogive) | L_n | 115 mm |
| Body tube length | L_b | 300 mm |
| Total mass (loaded) | m | 107.3 g |
| Number of fins (baseline) | N_f | 3 |
| Root chord (baseline) | C_r | 90 mm |
| Tip chord (baseline) | C_t | 30 mm |
| Semi-span (baseline) | s | 50 mm |
| Mid-chord sweep length (baseline) | l_m | 45 mm |
| Fin thickness ratio | t/c | 0.08 |
| Reference velocity | V | 60 m/s |

Six parametric studies were conducted from this baseline, each varying one fin-geometry variable while holding the others fixed as noted: (1) fin aspect ratio, with planform area and taper ratio held constant by simultaneously adjusting span and chords; (2) taper ratio, with span and planform area held constant; (3) leading-edge sweep angle, with span and chords held constant; (4) fin count (2, 3, 4, and 6 fins), repeated across the aspect-ratio sweep; (5) apogee sensitivity to aspect ratio, via the trajectory model of Section III; and (6) fin planform shape — trapezoidal, clipped-delta, and elliptical — compared at equal planform area and span. For the elliptical planform, the induced/interference drag reduction relative to a trapezoid of equal area is represented by an empirical factor of 0.90, consistent with wind-tunnel comparisons reported for elliptical versus straight-tapered fins [3], [6]. In every study the nose and body contribution ($C_{N\alpha,n} = 2$, $X_{cn} = 0.466 \cdot L_n$ for a tangent-ogive nose) and the airframe center of gravity were held fixed, so that reported changes in static margin isolate the effect of fin geometry alone.

## 5 RESULTS AND DISCUSSION

The baseline configuration of Table I yields a fin normal-force-coefficient slope of $C_{N\alpha,f} \approx 26.8$ per radian, a total vehicle $C_{N\alpha,total} \approx 28.8$ per radian, a center of pressure 339 mm from the nose tip, and a static margin of 3.43 calibers (Figure 2) — a comfortably stable, slightly conservative baseline consistent with a first-flight design philosophy [5].

### 5.1 Effect of Aspect Ratio

Figure 3 shows static margin and fin drag coefficient as the fin aspect ratio is varied from 0.6 to 3.5 while planform area, taper ratio, and fin count are held fixed. Static margin is nearly insensitive to aspect ratio, varying by less than 3% (peaking near AR ≈ 1.2 before declining slightly), because the Barrowman fin term in (1) trades an increasing $(s/d)^2$ term against an increasing sweep-related denominator as span grows at fixed area. Fin drag, by contrast, increases monotonically and substantially — approximately 19% — across the same range, because higher-aspect-ratio fins of fixed area have a longer effective wetted span exposed to the interference-drag term of (7). This indicates that, for a fixed planform area, aspect ratio is primarily a drag lever rather than a stability lever, and that low-to-moderate aspect ratios (AR ≈ 1–2) are preferable when apogee is a design priority.

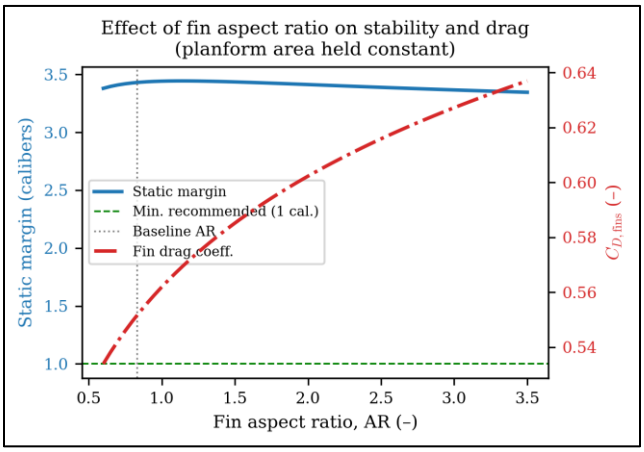


**Figure 3: Static margin (left axis) and fin drag coefficient (right axis) versus fin aspect ratio, at constant planform area, taper ratio, and fin count.**

### 5.2 Effect of Taper Ratio

Figure 4 shows static margin as a function of taper ratio $\lambda=C_t/C_r$, with span and planform area held constant. Static margin decreases monotonically as $\lambda\to 1$ (i.e., as the fin approaches a rectangular planform), because increasing tip chord shifts the fin's own center of pressure rearward relative to the root, but more importantly, at fixed span and area, a rectangular fin must reduce its root chord, moving the effective fin CP forward relative to a low-taper fin with a long root chord anchored at the aft body. Over the studied range the static margin falls from approximately 3.6 to 3.2 calibers, a change of similar magnitude to the aspect-ratio effect but acting in the opposite design direction. This confirms the common hobby-rocketry practice of favoring moderate-to-low taper ratios ($\lambda\approx 0.2$–$0.4$) for stability-critical designs [3], [5].

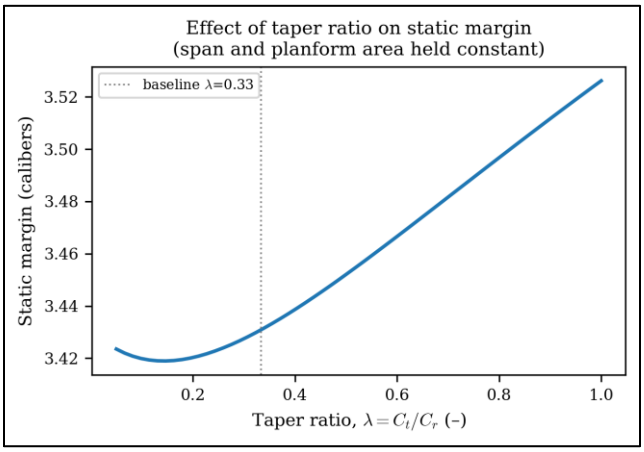


**Figure 4: Static margin versus fin taper ratio $\lambda=C_t/C_r$, at constant span and planform area.**

### 5.3 Effect of Leading-Edge Sweep Angle

Figure 5 shows static margin as the leading-edge sweep angle is varied from 0° to 60° with chords and span held fixed (so planform area is constant but l_m, and hence sweep, changes). Static margin is relatively flat for sweep angles below approximately 35°–40°, beyond which it declines more noticeably as the fin's center of pressure is carried aft relative to the body reference, altering the fin moment arm through the l_m term in (1) and (3). This suggests that moderate sweep can be used freely for structural or aesthetic reasons without materially compromising stability, but that designers seeking maximum static margin at fixed planform area should avoid highly swept, low-aspect-ratio ("delta-like") fins.

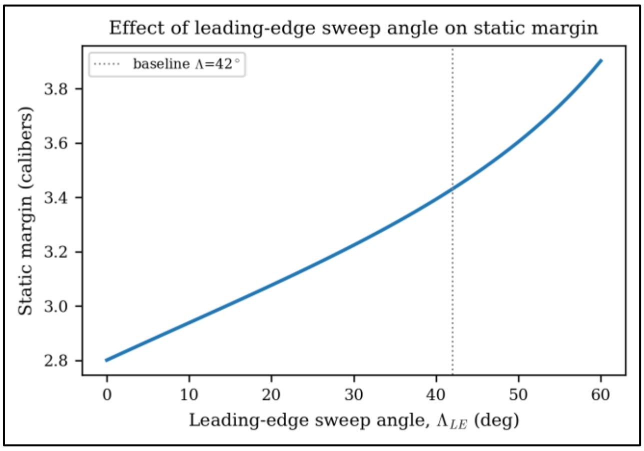


**Figure 5: Static margin versus leading-edge sweep angle Λ_LE, at constant fin chords and span.**

## 5.4 Effect of Fin Count

Figure 6 compares static margin and fin drag coefficient across the aspect-ratio sweep for 2, 3, 4, and 6 fins. Both quantities scale approximately linearly with fin count, since N_f enters (1) and (7) as a direct multiplier. Increasing fin count from 3 to 4 raises static margin by roughly one-third and fin drag by a comparable fraction; six fins very nearly double both relative to the three-fin baseline. Because stability requirements can typically be met with a smaller, lower-drag fin set, these results support the widely used convention that three or four fins represent the practical optimum for sport model rockets, with additional fins reserved for cases where roll damping or aesthetic/structural requirements outweigh the drag penalty [3], [4].

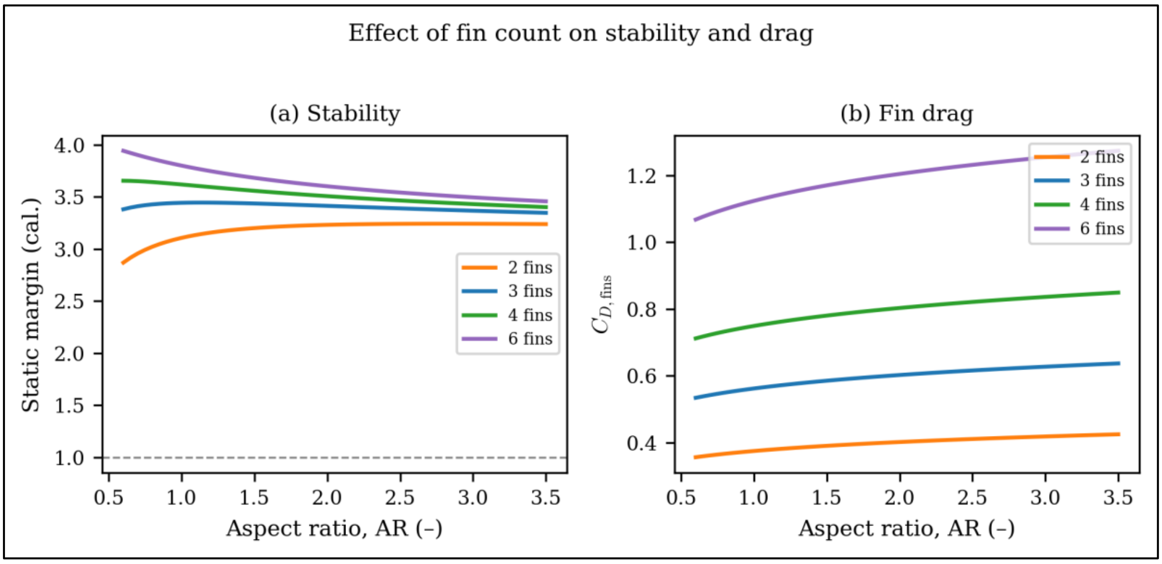


**Figure 6: Effect of fin count (2, 3, 4, 6) on (a) static margin and (b) fin drag coefficient, across the same aspect-ratio sweep as Figure 3.**

## 5.5 Effect on Predicted Apogee

Figure 7 shows the predicted apogee from the simplified trajectory model of Section III as fin aspect ratio is varied, using the corresponding fin-drag values from Figure 3 added to a fixed body/nose drag coefficient. Apogee decreases modestly but consistently with increasing aspect ratio, from approximately 151 m to 148 m over the studied range — a relative altitude loss of about 2.5% attributable to fin drag alone. While the absolute values depend on the simplified propulsion and drag assumptions and should not be read as flight predictions for a specific motor, the trend confirms that the aspect-ratio drag penalty identified in Section V-A propagates directly into a measurable, if secondary, altitude cost, reinforcing that aspect-ratio selection should weigh drag more heavily than stability for this vehicle class.

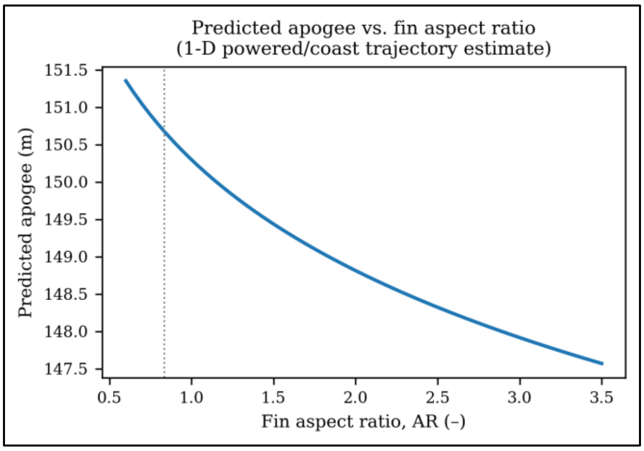


**Figure 7: Predicted apogee versus fin aspect ratio, from the simplified one-dimensional powered/coast trajectory model.**

### 5.6 Effect of Fin Planform Shape

Figure 8 shows the fin outlines and Figure 9 compares static margin and fin drag coefficient for trapezoidal, clipped-delta, and elliptical planforms of equal area and span. The clipped-delta fin achieves the highest static margin of the three (by virtue of its long root chord anchoring the fin CP close to the body), closely followed by the trapezoidal baseline, while the elliptical fin yields the lowest static margin (approximately 8% below the trapezoidal case) but also the lowest drag coefficient (approximately 10% below the trapezoidal case), consistent with the reduced tip and interference losses long associated with elliptical planforms in wind-tunnel studies of low-speed lifting surfaces [3], [6]. This highlights a genuine design trade-off: elliptical fins are attractive when apogee is prioritized and the resulting static margin remains within the acceptable range, whereas clipped-delta or trapezoidal fins are preferable when maximum stability margin — for example, for a first flight or an unusually aft center of gravity — is the primary concern.

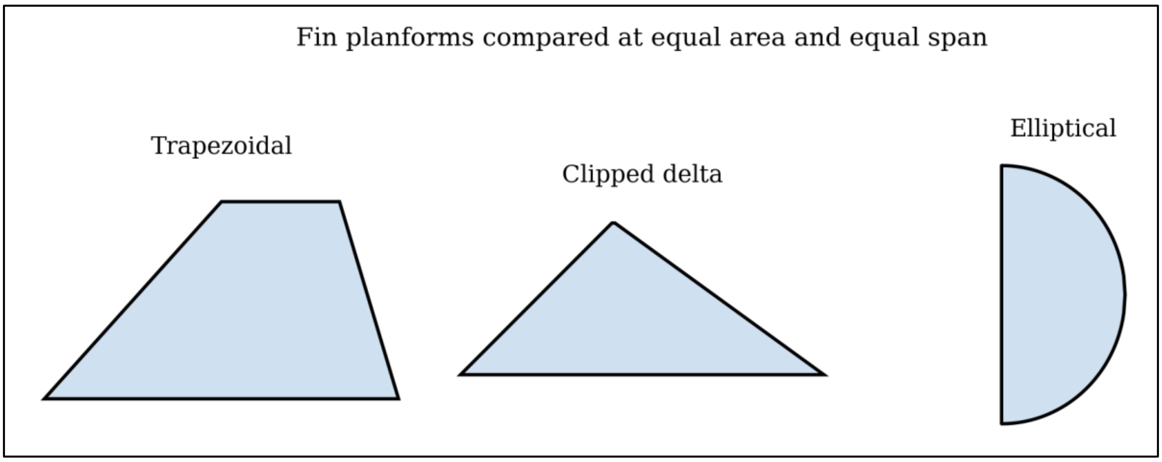


**Figure 8: Trapezoidal, clipped-delta, and elliptical fin planforms compared at equal area and equal span.**

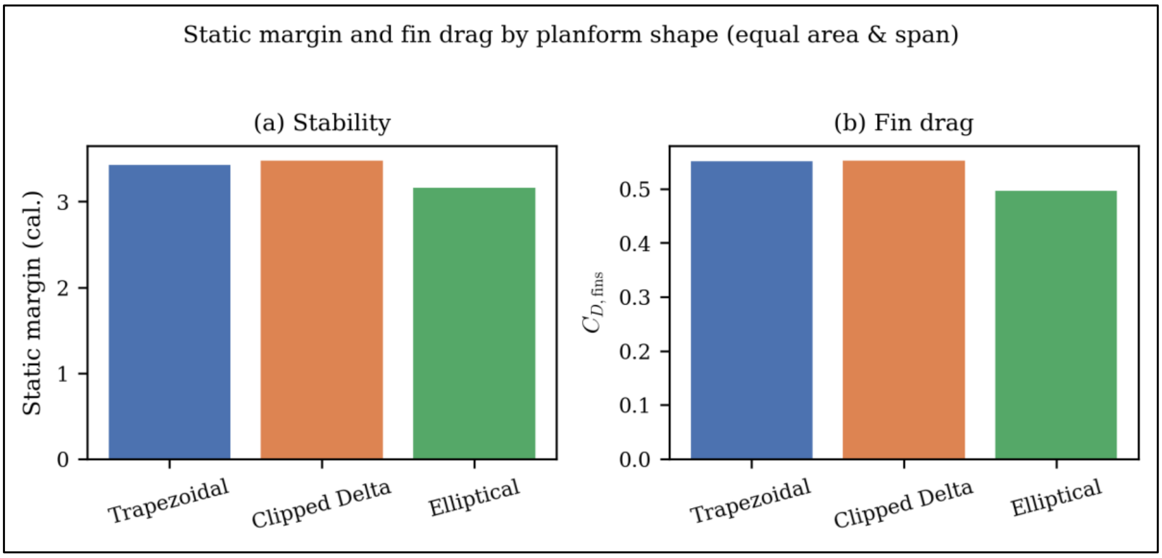


**Figure 9: (a) Static margin and (b) fin drag coefficient for the three planform shapes of Figure 8.**

## 6 DESIGN GUIDANCE

Table II consolidates the parametric results of Section V into practical guidance for selecting fin geometry. The general pattern that emerges is that stability is governed primarily by fin count, taper ratio, and sweep angle, while drag (and, through it, apogee) is governed primarily by aspect ratio, fin count, and planform shape. Because fin count and, to a lesser extent, aspect ratio influence both stability and drag in the same direction, they represent the two variables most worth iterating on for a given design: a designer can typically reach the desired static margin with the smallest, lowest-aspect-ratio fin set that meets the 1–2 caliber guideline, then adjust taper ratio and planform shape to fine-tune drag without materially compromising stability.

It should be emphasized that the quantitative trends above are specific to the baseline airframe of Table I; the Barrowman equations (1)–(5) and the drag model (6)–(7) are, however, general, and the same methodology can be applied directly to any other body diameter, mass, or motor class by substituting the corresponding baseline values.

**Table 2 Summary of Fin-Geometry Design Guidance**

| Fin variable | Effect on static margin | Effect on drag / apogee | Practical guidance |
|---|---|---|---|
| Aspect ratio ↑ | Slight increase then plateau (≈3.3–3.45 cal.) | Fin CD rises ~20% over AR 0.6→3.5 | Moderate AR (1–2) balances stability and drag |
| Taper ratio ↑ (Ct/Cr→1) | Decreases (CP moves forward) | Wetted area ~unchanged | Low λ (0.2–0.4) aids stability margin |
| LE sweep angle ↑ | Decreases steadily beyond ~40° | No direct CD effect (planform area fixed) | Moderate sweep preferred; avoid >45° if margin tight |
| Fin count ↑ (2→6) | Increases roughly linearly | CD increases roughly linearly | 3–4 fins is the practical optimum |
| Elliptical vs. trapezoidal | Slightly lower margin (~8%) at equal area | Lowest CD of the three shapes (~10% less) | Elliptical fins favored when drag/apogee is prioritized |

## 7 CONCLUSION

This paper applied the Barrowman method and a wetted-area drag model to systematically quantify the effect of fin aspect ratio, taper ratio, leading-edge sweep angle, fin count, and planform shape on the static stability and aerodynamic performance of a representative model rocket. Static margin was found to be comparatively insensitive to aspect ratio at fixed planform area, but sensitive to taper ratio, sweep angle, and — most strongly — fin count. Fin drag, and the corresponding apogee penalty, increased with both aspect ratio and fin count, and elliptical fins were shown to offer a measurable drag advantage over trapezoidal and clipped-delta planforms of equal area at a modest cost in stability margin. Taken together, the results support a practical design procedure in which fin count and taper ratio are used primarily to set static margin, while aspect ratio and planform shape are used to manage drag and altitude, and they provide a quantitative basis — beyond convention alone — for fin selection in student and hobby rocket projects. Future work could extend the present analytical treatment with computational fluid dynamics or wind-tunnel validation at the specific Reynolds numbers of interest, and could incorporate a full six-degree-of-freedom flight simulation to capture dynamic stability effects not addressed by the static-margin criterion used here.

## STATEMENTS ON COMPLIANCE WITH ETHICAL STANDARDS

### *Acknowledgments*

My profound appreciation goes to my, co-authors, colleagues, and mentors for their invaluable contributions, guidance, encouragement, and constructive feedback, which played a significant role in the successful completion and publication of this research work.

### *Disclosure of conflict of interest*

There is no conflict of interest to be disclosed.

## REFERENCES

[1] J. S. Barrowman and J. A. Barrowman, "The Theoretical Prediction of the Center of Pressure," National Association of Rocketry, NARAM-8 Tech. Rep., Aug. 1966.

[2] J. S. Barrowman, "The Practical Calculation of the Aerodynamic Characteristics of Slender Finned Vehicles," M.S. thesis, Dept. of Physics, Catholic Univ. of America, Washington, DC, USA, 1967.

[3] G. K. Mandell, G. J. Caporaso, and W. P. Bengen, Topics in Advanced Model Rocketry. Cambridge, MA, USA: MIT Press, 1973.

[4] S. Niskanen, "Development of an Open Source model rocket simulation software," M.S. thesis, Faculty of Information and Natural Sciences, Helsinki Univ. of Technology, Espoo, Finland, 2009.

[5] D. E. Fuller, "Effects of Nose Shape and Fin Geometry on Static Stability of a High-Fineness-Ratio Sounding Rocket," NASA Langley Research Center, Hampton, VA, USA, NASA Tech. Memo. TM X-1661, 1968.

[6] K. D. Harris, "Measurements of Lift, Drag and Pitching Moment on a Low-Speed Rocket Fitted with Tail Fins of Various Spans," College of Aeronautics, Cranfield, U.K., Rep. CoA/N-29, May 1955.

[7] N. B. Jampi and M. F. Zulkafli, "The Effect of Moveable Fins on Trajectory and Aerodynamic Characteristics of Model Rockets," J. Power and Aerospace Applied Technology, Universiti Tun Hussein Onn Malaysia, 2024.

[8] G. H. Stine and B. Stine, Handbook of Model Rocketry, 7th ed. Hoboken, NJ, USA: Wiley, 2004.

[9] J. D. Anderson, Jr., Fundamentals of Aerodynamics, 6th ed. New York, NY, USA: McGraw-Hill Education, 2017.

[10] G. P. Sutton and O. Biblarz, Rocket Propulsion Elements, 9th ed. Hoboken, NJ, USA: Wiley, 2017.

[11] National Association of Rocketry, "High Power Rocketry Safety Code," NAR, Marion, IA, USA. [Online]. Available: https://www.nar.org

[12] NASA Glenn Research Center, "Rocket Stability," Beginner's Guide to Rockets. [Online]. Available: https://www.grc.nasa.gov